gPCE Uncertainty Quantification Modeling of LiDAR for Bathymetric and Earth Science Applications*

Alexandra K. Wise^{1[0000-0002-3092-8833]}, Kevin W. Sacca^{1[0000-0002-6829-7707]}, and Jeff P. Thayer^{1[0000-0001-7127-8251]}

University of Colorado, Boulder, CO 80303, USA, Alexandra.Wise@Colorado.edu

Abstract. Most LiDARs, though precise, are vulnerable to position and pointing errors and, while fidelity of location/pointing solutions can be extremely high, determination of uncertainty remains relatively basic. As a result, NASA's 2021 Surface Topography and Vegetation (STV) Incubation Study Report lists vertical, horizontal, and geolocation accuracy as an associated Science and Application Traceability Matrix product parameter for most identified Science and Application Knowledge Gaps [5]. Currently, standard uncertainty quantification (UQ) approaches are plagued by simplifying approximations, ignored covariances, as well as improperly modeled (often exclusively Gaussian) uncertainty sources. The presented generalized Polynomial Chaos Expansion (gPCE) based method has wide ranging applicability to improve vertical, horizontal positioning and geolocation uncertainty estimates, for all STV disciplines, by more completely describing total aggregated uncertainties, from system level to geolocation, and intrinsically accounting for covariance between variables (without the need to manually construct a covariance matrix). gPCE also does not rely on many of the simplifying assumptions used in standard methods. Most importantly, it supports a number of additional (non-Gaussian) uncertainty sources, and arbitrarily high orders of variable cross-moments. gPCE is presented here, for the bare Earth case, as a proof of concept.

Keywords: Uncertainty Quantification · Bathymetric Lidar · TPU.

1 Motivation

NASA's 2021 Surface Topography and Vegetation (STV) Incubation Study Report lists vertical, horizontal, and geolocation accuracies as an associated Science and Application Traceability Matrix product parameter for most, identified Science and Application Knowledge Gaps, highlighting one of the primary shortcomings of modern LiDARs [5]. Though the precision instrument location, pointing, and, subsequent, geolocation capabilities of modern LiDAR systems is very high, many systems are vulnerable to position and pointing errors, as

^{*} Supported by NASA FINESST Award #80NSSC19K1351 and #80NSSC21K1597.

even small deviations from the expected principal axis lead to projection errors on target [3, 1, 2]. Currently, Uncertainty Quantification (UQ) remains relatively basic or non-existent for most instruments. This is, likely, due to the difficulty posed by determining uncertainties and the dubious fidelity of common methods, such as Total Propagated Uncertainty (TPU) and variations thereof. In fact, a known issue (since 2019) of the ICESat-2 Global Geolocated Photon data set (ATL03) has been the lack of dynamically calculated uncertainty estimates [4]. TPU methods, while computationally tractable, are often plagued by simplifying approximations and ignored covariances, potentially leading to under- or over-reporting of uncertainty estimates. Additionally, uncertainty sources are often exclusively modeled as Gaussian, inaccurately capturing some variable distributions, e.g., in the case of bathymetric LiDARs, wave spectral distributions are better described by Gamma distributions, which are supported under gPCE.

The presented research addresses specific knowledge gaps in LiDAR measurement uncertainty through a more complete description of total aggregated uncertainties, from system level to geolocation, by applying a generalized Polynomial Chaos Expansion (gPCE) based UQ approach. This method has wide ranging applicability to improve vertical and horizontal positioning, and geolocation uncertainty estimates, for all STV disciplines. gPCE can do so, by accounting for a number of factors, including covariances between variables (without manually constructing a covariance matrix), by properly representing input variable uncertainty distributions, and by minimizing the number of required simplifying assumptions. This is done by constructing and analyzing a surrogate model of the LiDAR system and its components (including platform), and subsequently applying the results of the model to the data directly. In a sense, gPCE can be thought of as a combination of Monte Carlo (MC) and TPU methods, in which the LiDAR system is modeled over a range of possible inputs (as in MC methods), the results are analyzed and converted into a set of equations which can propagate uncertainties, then these equations (as in TPU) are used to calculate individual uncertainties for each point in a point cloud. Point-wise positioning uncertainty determination using gPCE is less computationally expensive than Monte Carlo methods, and more tractable for most dimensionalities of interest (roughly from 3 to 20+ input variables). gPCE also does not rely on simplifying assumptions used in typical TPU methods (most importantly, a number of non-Gaussian uncertainty sources, and, an arbitrarily high order of variable cross-moments, can be represented). Finally, a key attribute of this approach is that global sensitivity analysis (GSA), after obtaining gPCE coefficients, is trivial and nearly costless to compute. GSA of system configurations/uncertainty is a powerful tool to design and develop LiDAR systems with the measurement requirements integrated directly into the design solution, as well as in the efficient operation and management of pre-existing LiDAR systems. gPCE is presented here, for the bare-Earth use case, as a proof of concept, with plans to expand to a bathymetric use case to demonstrate technique advantages due to complexities introduced by wave structure, roughness, entry angle, and water refractive index.

2 generalized Polynomial Chaos Expansion

$$\hat{\vec{u}}(\vec{y}) = \sum_{i=0}^{P} c_{\vec{j}_i} \Psi_{\vec{j}_i}(\vec{y}) + \epsilon_{\hat{\vec{u}}}$$

$$\tag{1}$$

A more detailed discussion of gPCE will take place during this paper's session. The generalized Polynomial Chaos Expansion, shown in Eq. 1, can be thought of as analogous to the more familiar Fourier Series expansion. It consists of a truncated infinite series of coefficients, $c_{\vec{j}_i}$, and orthogonal basis functions, $\Psi_{\vec{j}_i}$ (more accurately speaking, however, it is a Karhunen-Loève Expansion, with error in the expansion $\epsilon_{\hat{u}}$). The basis functions, as shown in Eq. 2, are the product of a number of Askey polynomial functions (of varying order) in a given variable (different Askey polynomials are chosen for different variable distributions).

$$\Psi_{\vec{j}_i}(\vec{y}) = \psi_{j_{i,1}}(y_1) \cdot \psi_{j_{i,2}}(y_2) \cdot \dots \cdot \psi_{j_{i,d}}(y_d)$$
 (2)

The ability to use multiple, and different, basis functions for different input variables, y_i , allows gPCE to avoid the assumption that all variables are Gaussian-distributed, and is central to the convergence of the method. In this investigation, we make the choice to represent input variables in the form $y_i = x_i + \omega_i$, such that the deterministic and stochastic components of each input can be treated individually. This allows us to numerically integrate (computationally efficiently, thanks to gPCE's properties) over all stochastic components at particular deterministic components (data points), in order to find the error in a given measurement.

$$\underbrace{\vec{y}_{1}}_{\text{input Samples}} \underbrace{\underbrace{\frac{\text{LiDAR System}}{\text{Simulations}}}}_{\text{Solution Samples}} \underbrace{\vec{u}(\vec{y}_{1})}_{\text{Invert to find } c_{\vec{j}_{i}}} \underbrace{\hat{u}(\vec{y})}_{\text{LiDAR Data}} \hat{x}_{ph}, \sigma_{\hat{x}}, \dots$$

$$\underbrace{\vec{v}_{K}}_{\text{Invert to find } c_{\vec{j}_{i}}} \underbrace{\hat{u}(\vec{y})}_{\text{LiDAR Data}} \hat{x}_{ph}, \sigma_{\hat{x}}, \dots$$
(3)

Though it is possible to solve for $c_{\vec{j}_i}$, the expansion coefficients directly, this approach tends to be difficult due to the large number of terms in the expansion. However, similar results can be had with other methods, such as inversion. In this investigation, the work-flow shown in Eq. 3 is used: First, a large number of input samples is generated, then solution samples are calculated from these inputs (using the same algorithm as might be applied to real data), and finally, the basis functions are calculated at the input samples and the system is inverted to find the coefficients. Once the gPCE model is found, it (or a truncated version of it) can then be applied to the real lidar data, and the model can be used to calculate the quantities of interest, such as the "bounce-point" location, the error in that value and other quantities of interest, at little computational cost.

3 Preliminary Topographic LiDAR gPCE Results

Results presented here were generated with the gPCE method introduced in the previous section, using the best analog for the ICESat-2 Photon Bounce

4 A. Wise, et al.

Point Geolocation Algorithm we could generate (and compare to actual ICES at-2 data), without direct access to either the ICES at-2 raw data or algorithm. Certain simplifications to this algorithm were made, e.g. atmospheric delay correction is not calculated, in order to advance this proof of concept. ICES at-2 ATL02 and ATL03 data were used to inform the input variable ranges in order to generate input variable samples. Due to space constraints, this section contains only a brief overview of the most important results generated.

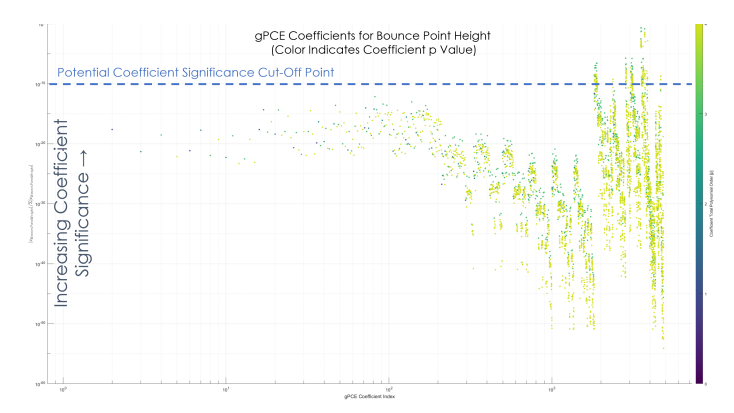


Fig. 1. gPCE coefficient significance for ICESat-2 Photon Bounce Point Height (above WGS84), colors indicate coefficient polynomial order (violet=0-th to yellow=4th order).

The gPCE technique, while still being actively developed and improved for use with LiDAR systems, yielded several results indicating the potential utility of the technique: Figure 1, shows the relative significance of gPCE coefficients, generated by this technique, for the photon bounce point location height component. Note the large difference between the most and least significant terms (≈ 50 orders of magnitude). In fact, only approximately 40 terms of 4850 had a relative significance greater than 1 ppm, indicating that the gPC-Expansion achieved satisfactory convergence, and that a further truncated expansion (with small terms removed) can still yield a high fidelity solution (one potential significance truncation point is shown at the 100 ppt significance level).

A further significant result, show in Fig. 2, is the ability of this technique to generate a high fidelity assessment of input-output parameter relationships. Showing the same data points as Fig. 1, Fig. 2 has been changed to display the total order in any given input parameter via the color of each point, as one might be interested in for design purposes, and shows a few interesting results. Namely, that the roll, pitch, and yaw pointing angles (and their uncertainties), show a greater significance level than the spacecraft position (in Earth-Centered Inertial Coordinates). The yaw pointing angle result, in particular, is a surprising one, given that the ICESat-2 instrument is a near-nadir pointing instrument, which intuitively should not be significantly impacted by yaw errors; this result is likely due to the slight, off-nadir components introduced by pitch and roll angles, which introduce a beam sweeping effect when the yaw angle is changed.

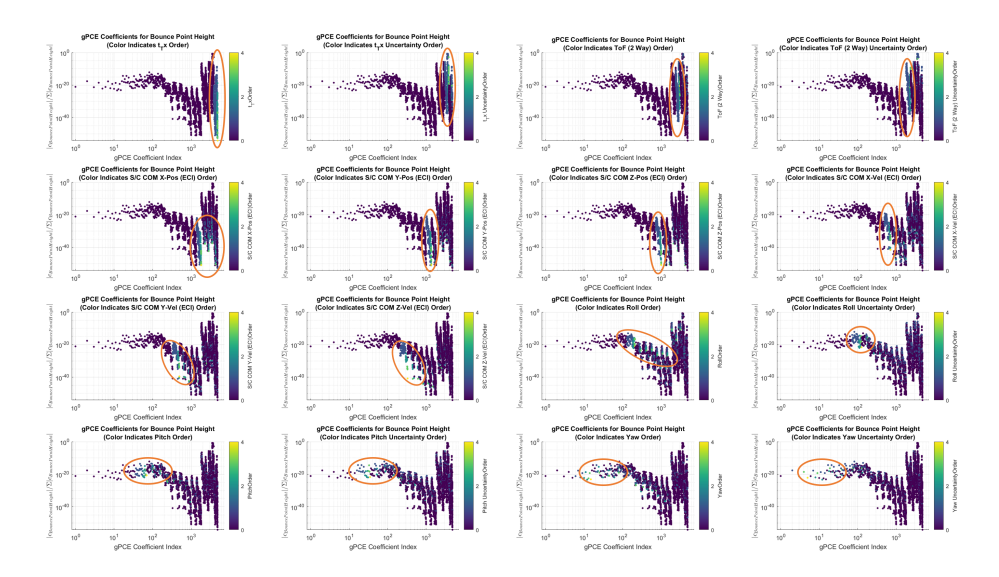


Fig. 2. gPCE coefficient relative significance for ICESat-2 Photon Bounce Point Height (above WGS84), colors indicate coefficient polynomial order in a given variable (violet=constant in a given variable, yellow=4th order in a given variable).

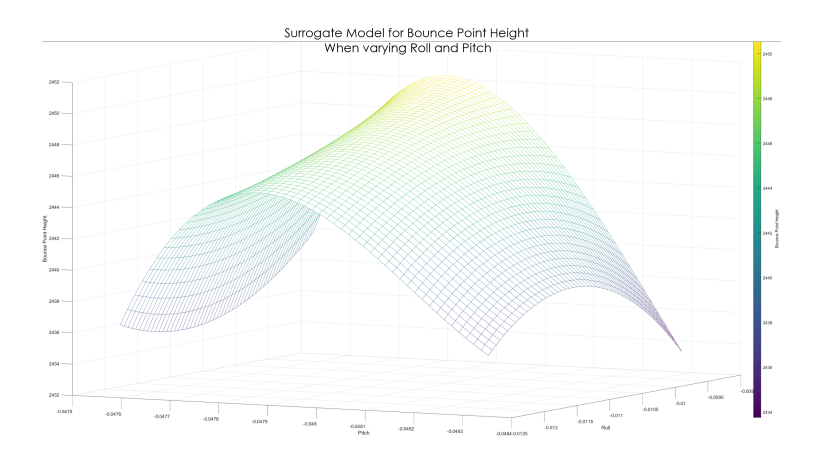


Fig. 3. gPCE model evaluated at a single data point with all variables held constant except roll and pitch, to show bounce point height sensitivity to roll, pitch, and roll+pitch effects. (Roll, pitch ranges kept broad for illustrative purposes.)

Fig. 3 shows an important capability of the gPCE technique, namely that various relationships between variables can be individually investigated. The gPCE bounce point height is evaluated at a particular set of input variables, which are all held constant, except for roll and pitch, which are allowed to vary. The resulting figure allows us to inspect visually the effect of the errors in each of these variables and how they are related; for example, near the center of the

figure, a given set of roll and pitch will clearly result in a much smaller height error, than at any of the four corners of this figure. Of additional interest is the fact that unlike the intuitive, bowl-shaped figure that may be expected when roll, pitch are varied (and ToF is held constant), the saddle shape shown in Fig. 3 more closely matches the physics of the ATLAS Photon Bounce Point Geolocation Algorithm. Specifically, ICESat-2's velocity (and associated motion during the photon ToF) requires that the length of each leg of the round trip be allowed to vary independently, causing this effect.

4 Concluding Remarks

gPCE, with it's ability to model covariances (as well as higher order cross-moments), it's reduced set of assumptions (over commonly used methods), and it's ability to natively represent non-Gaussian error sources, shows promise to improve vertical, horizontal, and geolocation accuracy for a wide range of STV disciplines. Meanwhile, all of this is accomplished with a technique and code that is portable and extensible to a wide variety of systems, platforms, and LiDAR processes and data products (e.g., bathymetric, atmospheric, topographical data, etc.) to enhance existing scientific returns and optimize future research.

Acknowledgments The Authors would like to thank Professor Alireza Doostan, for his assistance in applying the gPCE Method to Air- and Spaceborne Topo-Bathymetric LiDAR Measurements, and the NASA FINESST Program for funding support via NASA FINESST Awards #80NSSC19K1351 and #80NSSC21K1597.

References

- Bae, S., Helgeson, B., James, M., Magruder, L., Sipps, J., Luthcke, S., Thomas, T.: Performance of ICESat-2 Precision Pointing Determination. Earth and Space Science 8(4), 1-8 (2021). https://doi.org/10.1029/2020EA001478
- Luthcke, S.B., Thomas, T.C., Pennington, T.A., Rebold, T.W., Nicholas, J.B., Rowlands, D.D., Gardner, A.S., Bae, S.: ICESat-2 Pointing Calibration and Geolocation Performance. Earth and Space Science 8(3), 1–11 (2021). https://doi.org/10.1029/2020EA001494
- 3. Luthcke, S.B., Zelensky, N.P., Rowlands, D.D., Lemoine, F.G., Williams, T.A.: The 1-centimeter orbit: Jason-1 precision orbit determination using GPS, SLR, DORIS, and altimeter data. Marine Geodesy **26**(3-4), 399–421 (2003). https://doi.org/10.1080/714044529
- 4. Neumann, T.A., Brenner, D., Saba, Α., Hancock, Robbins, Gibbons, J., Harbeck, Κ., Α., Lee, J., Luthcke, S.B., Rebold, Т., ICESat-2 ATL03 Known Tech. Issues. 2021, NASA (2021),https://nsidc.org/sites/nsidc.org/files/technicalreferences/ICESat2 ATL03 Known Issues v004.pdf
- 5. Surface Topography and Vegetation Incubation Study Team: Observing Earth's Changing Surface Topography & Vegetation Structure. Tech. rep., NASA (2021)